INTERNATIONAL SOCIETY FOR SOIL MECHANICS AND GEOTECHNICAL ENGINEERING



This paper was downloaded from the Online Library of the International Society for Soil Mechanics and Geotechnical Engineering (ISSMGE). The library is available here:

https://www.issmge.org/publications/online-library

This is an open-access database that archives thousands of papers published under the Auspices of the ISSMGE and maintained by the Innovation and Development Committee of ISSMGE.

The paper was published in the proceedings of the 7th International Young Geotechnical Engineers Conference and was edited by Brendan Scott. The conference was held from April 29th to May 1st 2022 in Sydney, Australia.

Coupling effects of particle shape and internal pores on the mechanical properties of calcareous sand

Effets de couplage de la forme des particules et des pores internes sur les propriétés mécaniques du sable calcaire

Yaru Lv, Xin Li & Yuchen Su

College of Mechanics and Materials, Hohai University, China, yaru419828@hhu.edu.cn.

Jinabo Su

College of Harbour, Coastal and Offshore Engineering, Hohai University, China

ABSTRACT: Calcareous sand is a typical problematic marine sediment because of various shapes and complex internal pores in sand particles. The coupling effects of particle shape and internal pores on the mechanical properties of calcareous sand particles have rarely been investigated. This paper reconstructs calcareous sand particles including the apparent shape and internal structure by X-ray Computed Tomography Imaging, finding that calcareous sand particles are irregular in shape and include developed internal pores with the porosity ranges from 1.50% to 15.83%. The mechanical behavior was studied by particle compression tests and 3D discrete element analyses. The macro particle strengths of bulky, angularis, dendritic and flaky parties are 9.21, 6.69, 2.16, and 4.48 MPa, respectively. As the porosity is increased, the failure of particles gradually changes from tensile failure to compressive failure. The effects of porosity are larger than those of pore size, particularly for irregular dendritic and flaky particles. This is because the locations of fracture surfaces are firstly determined by particle shape, i.e., regular particle broken from loading points but irregular particles broken from the location subjected to the maximum bending moment, and then the crush mode is determined by pore size.

RÉSUMÉ: Le sable calcaire est un sédiment marin problématique typique en raison des formes variées et des pores internes complexes des particules de sable. Les effets de couplage de la forme des particules et des pores internes sur les propriétés mécaniques des particules de sable calcaire ont rarement été étudiés. Cet article reconstitue des particules de sable calcaire, y compris la forme apparente et la structure interne par la tomographie en rayons X. Il montre que les particules de sable calcaire ont une forme irrégulière et comprennent des pores internes développés dont la porosité varie de 1,50 % à 15,83 %. Le comportement mécanique est étudié par des tests de compression en particules et des analyses par éléments discrets en 3D. Les résistances macro-particulaires des parties volumineuses, angulaires, dendritiques et floconneuses sont respectivement de 9,21, 6,69, 2,16 et 4,48 MPa. Lorsque la porosité augmente, la rupture des particules passe progressivement de la rupture en traction à la rupture en compression. Les effets de la porosité sont plus importants que ceux de la taille des pores, en particulier pour les particules irrégulières dendritiques et floconneuses. Ceci s'explique par le fait que les surfaces de rupture sont d'abord déterminés par la forme des particules, c'est-à-dire que les particules régulières se brisent à partir des points de chargement, mais les particules irrégulières se brisent à partir de l'endroit soumis au moment de flexion maximal, puis le mode d'écrasement est déterminé par la taille des pores.

KEYWORDS: calcareous sand; particle shape; internal pore; crushing stress.

1 INTRODUCTION

The mechanical properties of sand particles are controlled by a number of factors, in which particle shape and internal flaw are important factors. Shape of particles is commonly represented by sphericity, roundness and smoothness (Cho et al. 2006), which are used to characterize a common shape, but difficult for particles with very irregular shapes. Because spherical particles roll faster than irregular, the roll-lock coefficient related to surface area and volume is adopted to describe the rollability (Latham et al. 2008). In shape classification, sphericity, surface area and volume of particle are available and effective (Xu and Chen, 2013). Internal flaw changes the crushing characteristics of ideal spherical particle (Lv et al. 2021). To date, few studies have reported the coupling effects of particle shape and internal pores, which is critical for geotechnical engineering, such as the calcareous sand in marine geotechnical engineering.

Calcareous sediment mainly exists in megathermal marine environments between 30 degrees of north latitude and 30 degrees of south latitude, e.g., the coastal shores of the Mediterranean, the Red Sea of Egypt, the Persian Gulf of Iran, and the South China Sea (Yu et al. 2006). As calcareous sand generally has high void ratio (e.g., external and internal voids), high compressibility and extreme crushability, its particle strength is a concerned topic. Jaeger (1967) proposed the

method to calculate the tensile strength of particle under quasi-static loading. Kwag et al. (1999) further improved it by considering the shape of calcareous sand. Particle strength of a sand have a characteristic strength according to the Weibull statics, which is a useful tool to analyze the strength of soil and rock particles (McDowell and Amon 2000). Besides the physical tests, discrete element method (DEM) is commonly used to simulate the mechanical behavior of particles (Lv et al. 2021; Cil et al. 2020), because it is superior in tests repeatability and variables controllable. Although the particle strength of calcareous sand has been studied and reported (Nakata et al. 1999; Kuang et al. 2020), the coupling effects of particle shape and interna pores are rarely considered.

This paper reports a series of particle compression tests and DEM simulations to explore the coupling effects of particle shape and internal pores. Several calcareous sand particles were reconstructed using X-ray computed tomography (X-CT) tests, quantifying the porosity and distribution of internal pores.

2 PARTICLE SHAPE AND INTERNAL PORES

To reveal the internal structure and quantify the porous of calcareous sand particles in detail, total of 28 calcareous sand particles (7 for each typical shape) were selected and scanned

by X- μ CT equipment. The particles were scanned by Diondo D2 with a resolution of 3 nm. The voltage and current are 100 kV and 100 mA in this test. Approximately 1600 graphs are collected every 0.225 degrees to complete a 360-degree scan. All of the gathered graphs were import software VG to reconstruct 3D skeletons and pores. Typical reconstructed particles and pore distribution are shown in Figure 1, namely sample 1, 2, 3 and 4. It should be noted that the scale bar used to describe the pore size in individual particle, which is a relative reference for one particle.

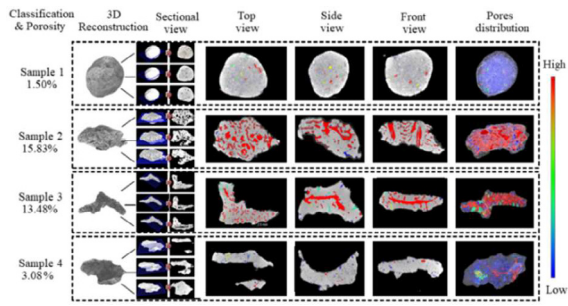


Figure 1. Typical reconstructed particles and pore distribution.

Because the ability of X-rays to penetrate material is inversely correlated with the atomic number, density and thickness of the medium, the gray parts and bright parts of the X-CT images represent the pores and skeleton of the calcareous sand particles, respectively. To clearly distinguish the pore and skeleton, color was used to quantify the pore size, the bigger the redder and the smaller the bluer. Take sample 3 as an example, there are many long channels with diameters ranging from approximately 90 μ m to 180 μ m. Channel branches are exposed to the side, indicating that the internal pores are very developed and well connected, forming a developed network of cavity. The percentage of the summarization of the pore volume to the total volume of the particle is defined as the internal porosity. The internal porosities of samples 1, 2, 3 and 4 are 1.50%, 15.83%, 13.48% and 3.08%, respectively.

3 MACROSCOPIC MECHANICAL PROPERTIES OF CALCAREOUS SAND PARTICLES

3.1 Photo-related particle compression tests

The particle compression tests were carried out by a traditional material test system with a maximum loading of 1 kN, as shown in Figure 2. During tests, the selected particles were placed onto the center of the bottom flat. Because the initial stable of particles governs the test results by changing the loading direction, the particles were rested on the longest dimension in physical tests according to the minimum potential energy, i.e., long axis of the particles is parallel to the plate. This stable will resist the initial rotation during loading as far as possible (Fu et al. 2017). During the tests, the top plate moved downward with a velocity of 0.5 mm/min until crushing occurred. The axial force and displacement were recorded in real time. The compression process was recorded by a camera with a rate of 240 frames/s. Additional lighting system was applied to improve the quality of photos (Todisco et al. 2017).



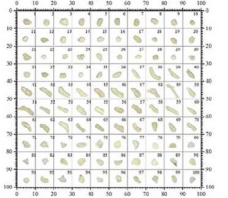


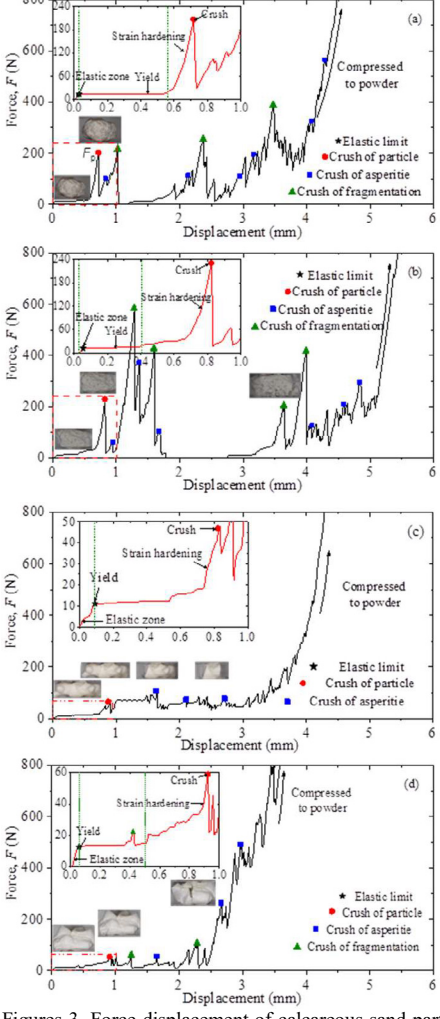
Figure 2. Setup of particle compression tests and samples.

Figure 2 also shows the particles chosen for the compression testing. The calcareous sand was sampled from Hainan Province, China. According to Latham et al. (2008), shape parameter of S/V distributes regionally for different shapes. Furthermore, an obvious stratification is found in the research of Asahina and Taylor (2011). In this paper, the coordinate system of sphericity and specific surface is adopted to describe the shape of calcareous sand particles. The sphericity is defined as the ratio of the diameter of the maximum inscribed sphere to the minimum circumscribed sphere, and specific surface is defined as the ratio of surface to volume. Sphericity and specific surface indicate the equiaxed and rolling-locking ability of particles, respectively. After analyzing the results of X-μCT, four typical shapes were adopted, i.e., bulky, angularis, dendritic and flaky. The sphericity of bulky is larger than 0.5, but that of the angularis is between 0.3 and 0.5. The shape of dendritic is utterly distant from that of flaky, but their sphericity are similar, which are smaller than 0.3. They are distinguished by specific surface, which is smaller than 2.70 for dendritic and larger than 2.70 for flaky.

3.2 Macroscopic strength of calcareous sand particles

Figures 3a, 3b, 3c and 3d show the typical measured force-displacement curves of calcareous sand particles with shapes of bulky, angularis, dendritic and flaky, respectively. As the loading is increased, the particles are compressed, resulting in elastic deformation, yielding, strain hardening and splitting. Almost all of the particles were observed to exhibit an elastic stage in the physical experiment, which was enlarged into the illustration later. The modulus of the elastic stage may be an important index to represent the mechanical properties of particles, such as the elastic modulus and marked elastic limit (yielding point). After the elastic stage, the yielding period occurs, which is followed by strain hardening. The yielding period lasts has a long duration. Further increasing the loading, the splitting occurred, corresponds to the peak values on the force-displacement curves. Small peaks indicate the fracturing of small asperities, which are not considered failure (McDowell and Amon 2000). Large peaks indicate the crushing of particle and fragmentations.

Agreeing with the results of Nakata et al. (1999), two typical failure modes were observed for calcareous sand. In mode I failure, the particle was continually compressed without obvious peak values in the force-displacement curve (i.e., without completely decline in axial force). Because the calcareous sand particle has a large number of incipient flaws, forming a complex and porous calcite skeleton, the particle skeleton failure initiated from the local loading point, extending to the whole particle. Meanwhile, a small amount of detritus was observed, and the quantity gradually increased; this detritus did not separate from the primary particle until the particle was compressed into powder. It can be observed from the morphological change that the typical characteristic of this failure is the result of the compression of internal pores, which is defined as compressive failure. In mode II failure, the force-displacement curves include many large and small peaks, like a sawtooth before final complete failure occurred. The sawtooth indicates the breakage of asperities and fragmentation, and the particles were broken into several fragments, including detritus. After splitting, classification (Saeidi et al. 2017) was observed (Lobo-Guerrero and Vallejio 2005), and some fragments separated from the breakage surface, as shown in the photographs. This failure is driven by tension and shearing and is defined as tensile failure. The crushing behavior was divided into the crushing of asperities and crushing of fragmentations. The first crushing of fragmentations is adopted in this paper.



Figures 3. Force-displacement of calcareous sand particles with shapes of (a) bulky; (b) angularis; (c) dendritic; (d) flaky

Particle crushing is considered as tensile failure. According to Nakata et al. (1999) and Kwag et al. (1999), particle strength is usually calculated as the crushing force divided by resisting area, as expressed by Equation 1:

$$\sigma = \frac{F}{hd} \tag{1}$$

where F is the first typical peak force; b and d are the initial size of resisting area for particles. For bulky particles, b and d are average diameter of three orthogonal directions; for angularis and dendritic particles, b and d are the middle and minimum dimensions, respectively; for flaky particles, b and d are the maximum and minimum dimensions.

Results of the crushing strength of calcareous sand particles with different shapes were further analyzed according to Weibull statics. The crushing stresses of particles with different shapes are illustrated in Figure 4. The particle strength distribution has significant differences between the four typical shaped particles. The characteristic strengths of bulky, angularis, dendritic and flaky parties are 9.21, 6.69, 2.16, and 4.48 MPa, respectively. As expected, the bulky particle has the highest strength because it is less affected by the irregularity. The angularis is the second only to bulky because of its irregularity. As illustrated by Wang and Coop (2016), particles with higher local roundness tend to break in explosive mode with higher strength, whereas the lower roundness tend to the asperity breakage with a lower strength. The characteristic strength of

dendritic particles is smallest. In addition, the broken of little coral branches also influence the fragmentation of the particle. The Weibull modulus are 1.8, 1.21, 0.83 and 1.61 for bulky, angularis, flaky and dendritic, respectively. The bulky has the largest strength and lowest dispersion, which is opposite to the dendritic. Compared to angularis, flaky has a larger Weibull modulus but smaller characteristic strength, which illustrates the characteristic strength of flaky is more centralized.

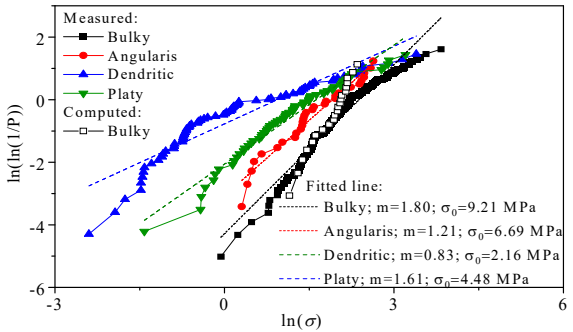


Figure 4. Weibull distributions of crushing strength.

The results of compression tests indicate that the particle strength has significantly differences between bulky, angularis, dendritic and flaky. This phenomenon may be caused by particle shape and/or internal pores because the porosity is associated with particle shape. However, the contributions are difficult to be quantified by physical tests because the porosity and distribution of internal pores are rarely determined.

4 MICROSCOPIC MECHANISM OF CALCAREOUS SAND PARTICLES

4.1 DEM numerical modeling and parameters

DEM numerical simulations were carried out using PFC3D 5.0 software (Itasca Consulting Group Inc 2015). The sand particles were simulated by a breakable cluster, which is the composition of rigid and unbreakable elementary balls. The reconstructed three-dimensional particles are imported acting as the particle boundary. The elementary balls were filled within the boundary and then bonded to simulate the calcareous sands with different outer morphology, as shown in Figure 5. Single particle is placed between two rigid walls. The upper wall moved downward at a constant speed to simulate the physical tests. Considering the calculation time and accuracy, Lv et al. (2021) studied the influence of compression velocity in simulate, finding that the crushing force is not apparently affected by the loading rate when it is smaller than 1 m/s. In addition, magnitude of the elementary balls also confirmed to exceed 500 (Lim and McDowell, 2007). In this study, the loading rate is 0.1 m/s, and approximately 3000-5000 elementary balls were adopted to simulate the crushable particles. According to Fu et al. (2017), linear parallel bond model and linear contact model were adopted in contact of ball-ball and ball-facet, respectively.

Linear parallel bond provides linear elastic frictional and cement-like behavior. The stiffness of normal $(\overline{k_n})$ and shear $(\overline{k_s})$ directions are calculated as follows:

$$\overline{k_n} = \frac{\overline{E^*}}{L} \tag{2}$$

$$\overline{\mathbf{k}_{\mathrm{S}}} = \frac{\overline{k_{n}}}{r_{k}} \tag{3}$$

where $\overline{E^*}$ is the effective modulus of the parallel bond. The contact force and moment of the parallel bond model update according to the force-displacement as follows:

$$F_{c} = F^{l} + F^{d} + \overline{F}$$

$$M_{c} = \overline{M}$$
(4)

$$M_{c} = \overline{M} \tag{5}$$

in which, \overline{F} is the parallel-bond force, \overline{M} is the parallel-bond moment. Once the normal or shear component exceeds the preassigned value, the parallel bond will break and invalid, then the linear part is used to calculate and update the contact force between the particles.

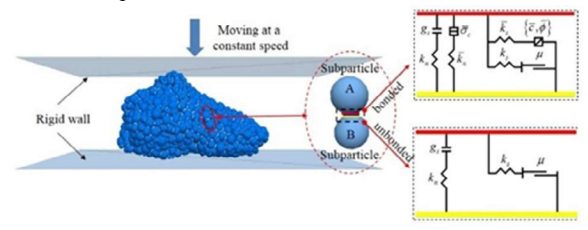


Figure 5. Typical DEM numerical simulation and adopted contact

Linear parallel bond provides linear elastic frictional and cement-like behavior, which is commonly used in BPM (Bond Particle Method) to simulate the crushing behavior of particle. Linear contact model is set between the wall and the elementary balls, meanwhile parallel bonding model was adopted for the inside of the breakable particles. These two models are linear-based models, which can only transmit force without torque. The cemented balls can withstand force and moment at the same time. If the distance between two balls is less than the set distance, a bonding bond will be formed. During loading progresses, when the force between the particles (tensile/force or shear force) is greater than the set value, the bonding bond will fail and degenerate into linearity. The model will degenerate to a linear model. The fracture simulation of the bonding bond also means the generation of particle breakage. The micro parameters of elementary balls and bonds are usually determined by trial and error. However, the macro mechanical behavior of particles is determined by the micro parameters of elementary balls and bonds in numerical simulation. The macro and micro parameters are relevant. For example, in an ideal condition that a particle consists of infinite elementary balls, summation of the tensile bond strength should be equal to the crushing force. As stated in physical experiments, the modulus of the elastic stage and the crushing stress represent the initial stiffness and crushing behavior of particles. In this paper, the modulus of the elastic stage is tried to characterize the effective modulus and the crushing stress is tried to characterize the tensile bond strength. The particle diameter (d), effective modulus (E* and \overline{E}^*), reference tensile bond strength ($\overline{\sigma}_{c,0}$), and cohesion (\bar{c}) were assigned random values between the corresponding measured maximum and minimum values. The stiffness ratio (r_k) and friction coefficient (μ) were determined by referring to Cil et al. (2020). The installation gap (\bar{g}_i) and friction angle $(\bar{\varphi})$ were determined after trial and error. Specific parameters are summarized in Table.1.

The computed crushing stresses of bulky particles are also illustrated in Figure 4. The computed results agree well with the measured, indicating the reasonable of numerical model and parameters adopted.

4.2 Coupling effects of particle shape and porosity

Calcareous particles with typical shapes of bulky, angularis, dendritic and flaky are simulated by DEM, which results are illustrated in Figures 6a, 6b, 6c and 6d, respectively. Internal pores of particles were formed by removing some elementary balls and connected bonds in random. The internal porosity of a sand particle is determined by the sum of the volumes of all the removed balls divided by the total volume of the sand particle. In other words, the internal porosity is the ratio of the removed bonds to the total bonds. Six porosities of 5%, 10%, 15%, 20%, 25%, 30% are considered. In this figure, the force-displacement along with the cracked bonds and force chains at the time of particle crush are shown. As the loading is increased, the force-displacement curve almost moves downward. During the loading process, there are many large and small fluctuations, indicating the breakage of the asperities of the separated parts. More local failures are found for angularis and dendritic particles because those two types of particles have amount of little angularness and dendrites. The force-displacement curve clearly peaks (i.e., whole broken), indicating particle crushing.

flakv

Uniform parameters in all simulations	bulky	blocky	angularis	
Particle diameter (mm)	3.29-5.93	3.52-6.17	4.07-6.88	3

Table 1. Parameters adopted in numerical simulations.

simulations	bulky	ыоску	angularis	паку		
Particle diameter (mm)	3.29-5.93	3.52-6.17	4.07-6.88	3.06-5.85		
Minimum radius of elementary ball	0.02	0.02	0.02	0.02		
(mm) Maximum radius of elementary ball	0.2	0.2	0.2	0.2		
(mm) Density (kg/m ³)	2810	2810	2810	2810		
Linear group						
Stiffness ratio, r_k	2	2	2	2		
Friction coefficient, μ	0.5	0.5	0.5	0.5		
Effective modulus, E* (MPa)	3.94-140	1.33-23.43	13.8-282.4	6.3-107.6		
Parallel bond group						
Stiffness ratio, $\overline{r_k}$	2	2	2	2		
Installation gap, $\overline{g_i}$ (mm)	0.05	0.05	0.05	0.05		
Friction angle, $\bar{\boldsymbol{\varphi}}$ (°)	30	30	30	30		
Effective modulus,	3.94-140	1.33-23.43	13.8-282.4	6.3-107.6		
$\overline{E^*}(MPa)$						
Tensile strength, $\overline{\sigma_{c,0}}$ (MPa)	0.94-35.4	1.39-10.36	0.09-4.2	0.65-24.63		
Cohesion, \overline{c} (MPa)	0.94-35.4	1.39-10.36	0.09-4.2	0.65-24.63		

The broken mode is closed related to particle shape. For the regular bulky particle, the bond near the loading point or critical flaws breaks first and then extends to a surface. For the angularis particle, bonds in sharp corner near the loading point are first broken, resulting in several small fluctuations before whole crush. For irregular dendritic and flaky particles, the bonds subjected to obvious bending moments are broken first, meanwhile the particle shape is the governing factor. For the relatively dense particles (i.e., internal porosity of 5%), the bonds near loading point breaks first and then extends to a surface, which is the fracture surface. The broken bonds from plan view show that the particles are divided into several parts along the broken surfaces. This is typical tensile failure. With the increasing internal porosity, the broken bonds become more dispersed, indicating that compression failure occurs. In other words, as the porosity is increased, the failure of particles gradually changes from tensile failure to compressive failure. The various of particle strength with porosity is shown in Figure 7. For bulky and flaky particles, the particle strength logarithmically decreases with increasing porosity. The force chain is relatively dense and uniform. It is derived that porosity is the governing factor for them. For angularis and dendritic particles, the peak force on force-displacement curves occur with a platform, which indicates the accumulation of local failure. The relationship between peak value and porosity are non-monotonic because coupling effects of porosity and shape changes the weakest point of the particle. The force chain is sparse and nonuniform. The governing factor is particle shape.

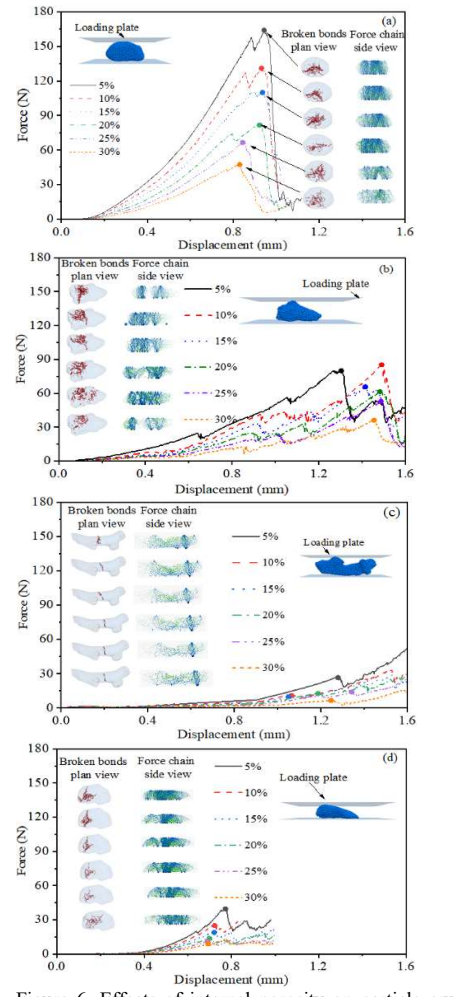


Figure 6. Effects of internal porosity on particle crush for calcareous sand with shapes of (a) bulky; (b) angularis; (c) dendritic; (d) flaky.

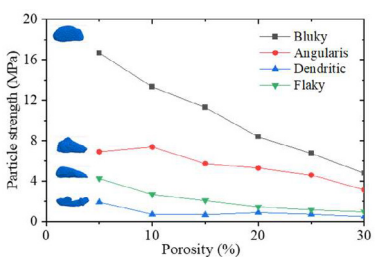


Figure 7. Variation of particle strength with porosity.

4.3 Coupling effects of particle shape and pore size

To investigate the coupling effects of particle shape and pore size, the size of the removed elementary balls is selected under a given internal porosity of approximately 10%. Five pore sizes are considered, which were determined by the dimension of the smallest side (d_{\min}) , i.e., $(0.025\pm0.016)d_{\min}$, $(0.035\pm0.007)d_{\min}$, $(0.045\pm0.003)\ d_{\min}$, $(0.055\pm0.002)\ d_{\min}$ and $(0.065\pm0.001)d_{\min}$, here, the elementary balls are removed in random. The force-displacement curves along with broken bonds and force chain are obtained and illustrated in Figure 8.

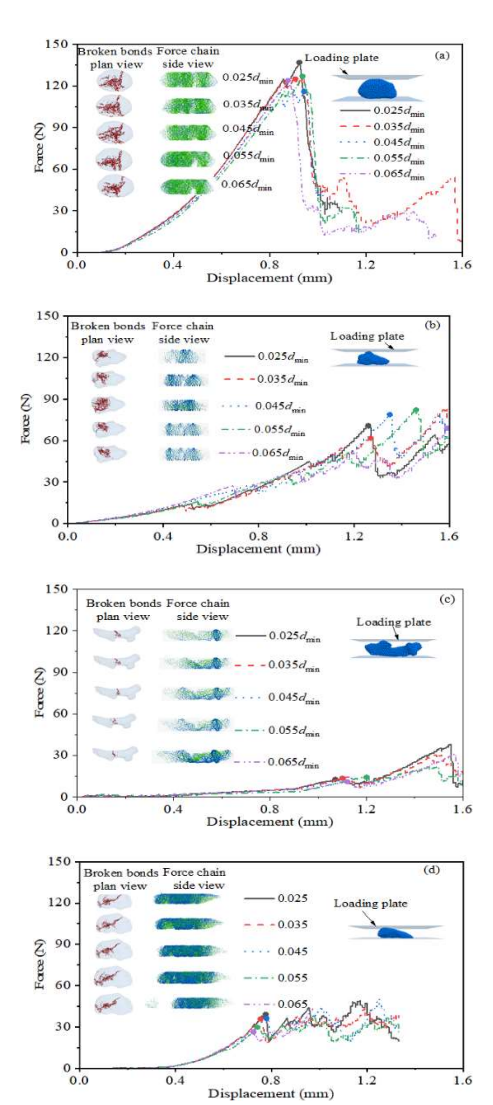


Figure 8. Effects of internal pore size on particle crush for calcareous sand with shapes of (a) bulky; (b) angularis; (c) dendritic; (d) flaky

The responses are different for particles with different shapes. From the side view of the force chain, the bulky particle is crushed from the loading point. The broken bonds concentrate to form a surface, and subsequently, the particle breaks along the surface. When the pore size ranges from $0.025\,d_{\rm min}$ to $0.065\,d_{\rm min}$, the disconnected force chain first increases and then decreases. From the plan view of the broken bonds, three fracture surfaces are developed. The particle is almost trisection, which is typical tensile failure. Particularly for the pore size of $0.045\,d_{\rm min}$, the included angles of three surfaces are approximately 120 degrees. The peak force exists a platform, which indicates that local fractures occur. Therefore, its particle strength is the smallest.

The effects of pore size on angularis particle are the biggest of the four shaped particles. Small peak values during loading (i.e., local fractures) are obviously changed by pore size. The reason is explored by the broken bonds and force chain. From the broken bonds, the fracture surfaces are also developed between the upper and lower loading points, but the particle is not broken in trisection. This is because the particle shape governs the crushing points. The fracture surface is obviously changed. For dendritic and flaky particles, fracture surfaces are not developed between loading points, but at the locations

subjected to bending moment. The locations of fracture surfaces are not changed with pore size, indicating that the effects of pore size are limited. As the pore size is increased, under a given internal porosity, large pores indicate a small number of pores, and vise verse. Larger pores may cause stress concentration, leading to tensile failure around the flaw. Therefore, the peak force decreases with the increasing pore size. The crushing stresses of the sand particles are illustrated in Figure 9. The crushing stress of bulky and angularis particles increases with pore size firstly and decreases, but that of the dendritic and flaky particles monotonic decreases. It indicates that crushing stress is governed by the combination of particle shape and pore size. The locations of fracture surfaces are firstly determined by particle shape, and then the crush mode is determined by pore size. In soil mechanics, the particle size distribution of soil affects its mechanical properties. Similarly, the pore size changes the particle size distribution of the elementary balls, thus influencing the simulated particle strength and stiffness. However, these are not monotonic correlations. Compared with the effects of internal porosity, the effects of pore size on the failure mode and particle strength are limited.

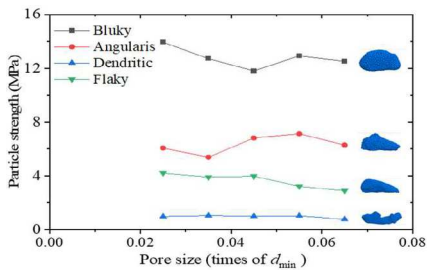


Figure 9. Variation of particle strength with pore size

5 CONCLUSIONS

This paper investigates the mechanical properties of porous calcareous sand by compression tests and discrete element analyses. The fragmentation mode, particle strength, effects of particle shape and internal voids are statistically analyzed. However, the influence of contact point between the particle and the loading plate is not considered. As an important factor of particle crushing, it will be studied in further experiments. In addition, our on-going investigations the role of real inner pore structures in particle crushing, which is particularly attractive for further understanding the properties of porous material. Based on the measured and computed results, some main conclusions are obtained as follows:

- (1) Calcareous sand particles are irregular in shape and include developed internal pores. The superficial pores extend inside the particles, forming a developed network of cavity. The internal porosity of the studied calcareous sand particles ranges from 1.50% to 15.83%.
- (2) Two typical failure modes are observed for calcareous sand particles. In compressive failure, the particles are continually compressed without an obvious rapid decline in axial force, where the particle skeleton is gradually compressed and forms small detritus. In tensile failure, the particles are broken into several fragments with obvious fracture surfaces, where the broken particle is classified by the several obvious peak values under the axial force. The characteristic strengths of relative regular bulky and angularis particles are larger than those of inregular dendritic and flaky particles.
- (3) The internal porosity has considerable effects on the mechanical properties, which reduces the strength of calcareous sand particles logarithmically. As the porosity is increased, the failure of particles gradually changes from

- tensile failure to compressive failure.
- (4) The effects of pore size are limited, particularly for irregular dendritic and flaky particles. This is because the locations of fracture surfaces are firstly determined by particle shape, i.e., regular particle broken from loading points but irregular particles broken from the location subjected to the maximum bending moment, and then the crush mode is determined by pore size.

6 ACKNOWLEDGEMENTS

The authors would like to acknowledge the support of the National Natural Science Foundation of China (No. 51779264) and the Central Universities fund operating expenses (No. B200202119).

7 REFERENCES

- Asahina D, Taylor MA. 2011. Geometry of irregular particles: Direct surface measurements by 3-D laser scanner. Powder Technology, 213(1-3), 70-78.
- Cho GC, Dodds J, Santamarina JC. 2006. Particle shape effects on packing density, stiffness, and strength: natural and crushed sands. J. Geotech. Geoenviron. Eng., 132, 591-602.
- Cil MB, Changbum S, Buscarnera G. 2020. DEM modeling of grain size effect in brittle granular soils. J. Eng. Mech. (ASCE), 146 (3), 04019138.
- Fu R, Hu X, Zhou B. 2017. Discrete element modeling of crushable sands considering realistic particle shape effect. Comput. Geotech., 91, 179-191
- Itasca Consulting Group Inc. 2015. PFC-Particle flow code, Ver. 5.0. Manual. Minneapolis: Itasca.
- Jaeger J. 1967. Failure of rocks under tensile conditions, International Journal of Rock Mechanics and Mining Sciences & Geomechanics Abstracts. 1967, pp. 219-227.
- Kuang DM, Long ZL, Guo RQ, Yu PY. 2020. Experimental and numerical investigation on size effect on crushing behaviors of single calcareous sand particles. Mar. Georesour. Geotec., 39 (2), 1-11.
- Kwag JM, Ochiai H, Yasufuku N. 1999. Yielding stress characteristics of carbonate sand in relation to individual particle fragmentation strength. Engineering for calcareous sediments. 1, 79-86.
- Latham JP, Munjiza A, Garcia X, Xiang JS, Guises R. 2008. Three-dimensional particle shape acquisition and use of shape library for DEM and FEM/DEM simulation. Minerals Engineering. 21, 797-805.
- Lim WL, McDowell GR (2007) The importance of coordination number in using agglomerates to simulate crushable particles in the discrete element method. Geotechnique, 57 (8), 701-705.
- Lobo-Guerrero R, Vallejio LE. 2005. Discrete element method evaluation of granular crushing under direct shear test conditions. J. Geotech Geoenviron Eng. 131, 1295-1300.
- Geotech. Geoenviron. Eng., 131, 1295-1300.
 Lv YR, Li X, Fan CF, Su YC. 2021. Effects of internal pores on the mechanicak properties of marine calcareous sand particles. Acta Geotechnica, 16, 3209-3228.
- McDowell GR, Amon A. 2000. The application of Weibull statistics to the fracture of soil particles. Soils and Foundation, 40 (5), 133-141.
- Nakata Y, Hyde AFL, Hyodo M, Murata H. 1999. A probabilistic approach to sand particle crushing in the triaxial test. Géotechnique, 49 (5), 567-583.
- Saeidi F, Yahyaei M, Powell M, Tavares LM. 2017. Investigating the Effect of Applied Strain Rate in a Single Breakage Event. Miner. Eng., 100, 211-222.
- Todisco MC, Wang W, Coop MR, Senetakis K. 2017. Multiple contact compression tests on sand particles. Soils Found., 57, 126-140.
- Wang W, Coop M. 2016. An investigation of breakage behaviour of single sand particles using a high-speed microscope camera. Géotechnique, 66 (12), 984-98.
- Xu WX, Chen HS. 2013. Numerical investigation of effect of particle shape and particle size distribution on fresh cement paste microstructure via random sequential packing of dodecahedral cement particles. Computers & Structures, 114-115, 35-45.
- Yu H, Sun Z, Tang C. 2006. Physical and mechanical properties of coral sand in the Nansha Islands. Mar. Sci. Bull., 8 (2), 31-38.